

- ⁶J. N. Shklyarevskii and R. G. Yarovaya, *Opt. Spektrosk.* **11**, 661 (1961) [*Opt. Spectrosc.* **11**, 355 (1960)].
- ⁷J. Toots, H. A. Fowler, and L. Marton, *Phys. Rev.* **172**, 670 (1968).
- ⁸N. Swanson, *J. Opt. Soc. Am.* **54**, 1130 (1964).
- ⁹R. E. LaVilla and H. Mendlowitz, *Appl. Opt.* **4**, 955 (1965).
- ¹⁰C. Herring and A. G. Hill, *Phys. Rev.* **58**, 132 (1940).
- ¹¹J. F. Cornwell, *Proc. R. Soc. A* **A261**, 551 (1961).
- ¹²T. L. Loucks and P. H. Cutler, *Phys. Rev.* **133**, A819 (1964).
- ¹³J. H. Terrell, *Phys. Rev.* **149**, 526 (1966).
- ¹⁴J. H. Tripp, P. M. Everett, W. L. Gordon, and R. W. Stark, *Phys. Rev.* **180**, 669 (1969).
- ¹⁵J. C. Kimball, R. W. Stark, and F. M. Mueller, *Phys. Rev.* **162**, 600 (1967).
- ¹⁶W. A. Harrison, *Phys. Rev.* **147**, 467 (1966); R. N. Gurzhi and G. P. Motulevich, *Zh. Eksp. Teor. Fiz.* **51**, 1220 (1966) [*Sov. Phys.-JETP* **24**, 1093 (1967)]; A. I. Golovashkin, A. I. Kopeliovich, and G. P. Motulevich, *Zh. Eksp. Teor. Fiz.* **53**, 2053 (1967) [*Sov. Phys.-JETP* **26**, 1161 (1968)].
- ¹⁷D. Brust, *Phys. Rev. B* **2**, 818 (1970).
- ¹⁸N. W. Ashcroft and K. Sturm, *Phys. Rev. B* **3**, 1898 (1971).
- ¹⁹R. V. Kasowski, *Phys. Rev.* **187**, 885 (1969).
- ²⁰L. W. Bos and D. W. Lynch, *Phys. Rev. B* **2**, 4567 (1970).
- ²¹P. A. Jaquet, *Metall. Rev.* **1**, 157 (1956).
- ²²W. C. Walker, D. M. Roessler, and E. Loh, *Phys. Rev. Lett.* **20**, 847 (1968).
- ²³E. Grüneisen and H. K. Adenstedt, *Ann. Phys. (Leipz.)* **31**, 714 (1938); E. Grüneisen and H. D. Erfiling, *Ann. Phys. (Leipz.)* **38**, 399 (1940).
- ²⁴T. Holstein, *Phys. Rev.* **88**, 1427 (1952); *Phys. Rev.* **96**, 525 (1954).
- ²⁵R. Fuchs and K. L. Kliewer, *Phys. Rev. B* **2**, 2923 (1970).
- ²⁶J. F. Cornwell, *Phys. Kondens. Mater.* **4**, 327 (1966).

PHYSICAL REVIEW B

VOLUME 7, NUMBER 8

15 APRIL 1973

Theory of Metal Surfaces: Induced Surface Charge and Image Potential

N. D. Lang

IBM Thomas J. Watson Research Center, Yorktown Heights, New York 10598

W. Kohn*

University of California, San Diego, La Jolla, California 92037

(Received 20 April 1972)

This paper contributes to the theory of the electron density distribution induced at a metal surface by a small static external charge distribution. As a first application, profiles of the charge induced by a uniform external electric field are obtained for metals of different bulk electron densities. A quantity of particular interest is the position of the center of mass, x_0 , of these profiles, for which we present numerical values. (The x axis is taken along the surface normal.) Next, the case of a small point charge q with x coordinate x_1 well outside the surface is treated. It is shown that the image potential experienced by such a charge has the form $-q^2/[4(x_1 - x_0)]$, where x_0 is the above-mentioned quantity. We locate x_0 , the effective position of the metal surface, relative to the last lattice plane of the crystal. We discuss the implications of these results for alkali adsorption on metal substrates, the capacitances of small-gap condensers, and field-emission experiments.

I. INTRODUCTION

In two previous papers^{1,2} we have developed a theory of metal surfaces, based on a density-functional formalism.^{3,4} We have applied this theory to calculations of the electron charge-density distributions, surface energies, and work functions of metal surfaces. These are all properties of unperturbed surfaces. In the present paper we add a discussion of the screening charges induced in a metal surface by the application of a uniform electric field or by the presence of an external point charge. These induced charges are familiar from elementary electrostatics. However, there they are idealized as being located on a mathematical surface of zero thickness. In reality they are of course spread out, extending over a thickness of the order of 2 \AA . The detailed nature of these in-

duced charge densities⁵ and its physical implications are the subject of the present paper.

The main contents of the paper are the following.

- (i) We formulate the general linear-response theory.
- (ii) We present the profiles of the additional surface-charge distributions induced by a uniform perpendicular electric field in metals of different bulk electron densities. In particular, we note the positions of the center of mass x_0 of these density distributions, relative to the positive charges, for various bulk electron densities.
- (iii) We show that, to a good approximation, the results of classical elementary electrostatics are valid, provided the idealized mathematical metal surface is taken to pass through x_0 . Thus the image potential for a charge q located at x_1 is given by

$$V^{im}(x_1) = -q^2/4(x_1 - x_0), \quad (1.1)$$

and the capacitance per unit area of a parallel-plate condenser is given by

$$C = \frac{1}{4\pi(x_0^{(a)} - x_0^{(b)})}, \quad (1.2)$$

where the superscripts refer to the two plates of the condenser.

(iv) We discuss the implications of these results for the positions of alkali ions adsorbed on metal surfaces, relative to the ion planes of the metal, for the capacitances of closely spaced condenser plates, and for the results of field-emission experiments.

II. SELF-CONSISTENT EQUATIONS

In this section we develop the necessary general theory of the linear response of metal electrons to an external⁶ static charge density. Several studies dealing with the response of metal-surface electrons to perturbing electric fields have recently been made.⁷⁻¹³ The present discussion differs from these in that it includes many-body effects, does not assume an infinite potential barrier at the surface, and includes quantitative results for charge-density profiles.¹⁴ We shall, in common with other authors, regard the positive charges as undisplaced by the external fields. *A posteriori*, we shall see that this is, in fact, a good approximation.

We shall use atomic units, $|e| = m = \hbar = 1$. In our previous papers^{1,2} we worked with the electron number density $n(\vec{r})$ and the electrostatic potential energy of an electron, $\phi(\vec{r})$. In the present paper, because of its close relationship with classical electrostatics, we shall work primarily with the charge density $\rho(\vec{r})$ and the electrostatic potential $\psi(\vec{r})$. Because of the negative charge of the electron,

$$\psi(\vec{r}) = -\phi(\vec{r}), \quad \rho(\vec{r}) = -n(\vec{r}). \quad (2.1)$$

The unperturbed electron density and uniform positive-charge background are shown schematically in Fig. 1. We employ the uniform-background model for the sake of simplicity. However, our principal results [Eqs. (3.9) and (4.12)] are also valid for a realistic metal, with a lattice of positive ions.

A. External Perturbing Potential

Since we are interested in linear response to external charges, it is sufficient to consider the effect of an external charge density of the form

$$\rho^{\text{ext}}(\vec{r}) = \delta(x - x_1)e^{i\vec{p}\cdot\vec{y}}, \quad (2.2)$$

where x_1 is well outside the electronic surface-charge cloud (see Fig. 1) and \underline{p} and \underline{v} are two-di-

mensional vectors,

$$\underline{p} = (p_y, p_z), \quad \underline{v} = (y, z). \quad (2.3)$$

The origin of the x axis is, for the present, an arbitrary point near the metal surface. The external potential generated by ρ^{ext} is, by Poisson's equation,

$$\psi^{\text{ext}}(\vec{r}) = \psi^{\text{ext}}(x; p)e^{i\vec{p}\cdot\vec{y}}, \quad (2.4)$$

where

$$\psi^{\text{ext}}(x; p) = (2\pi/p)e^{-p|x-x_1|}, \quad (2.5)$$

and $p \equiv |\underline{p}|$. For x in the region of the metal electrons, $x_1 - x$ is positive, so that (2.5) becomes

$$\psi^{\text{ext}}(x; p) = (2\pi/p)e^{-px_1}e^{px}. \quad (2.6)$$

B. Response Function

We are interested in the electron charge density induced by $\psi^{\text{ext}}(\vec{r})$ near the metal surface, which will screen this potential from the interior of the metal. This screening charge $\rho(\vec{r})$ may be regarded as linearly related either to the external perturbing potential $\psi^{\text{ext}}(\vec{r})$ or to the total perturbing potential

$$\psi(\vec{r}) \equiv \psi^{\text{ext}}(\vec{r}) + \int \frac{\rho(\vec{r}')}{|\vec{r} - \vec{r}'|} d^3\vec{r}'. \quad (2.7)$$

The latter is a more suitable choice, since physically the electrons are under the influence of the total potential. Hence we define the response function $K(\vec{r}, \vec{r}')$ by the equation^{7,8}

$$\rho(\vec{r}) = \int K(\vec{r}, \vec{r}')\psi(\vec{r}')d^3\vec{r}'. \quad (2.8)$$

Because of the translational and rotational invariance in the y - z plane, we may write

$$\psi(\vec{r}) = \psi(x; p)e^{i\vec{p}\cdot\vec{y}}, \quad (2.9)$$

$$\rho(\vec{r}) = \rho(x; p)e^{i\vec{p}\cdot\vec{y}}, \quad (2.10)$$

$$K(\vec{r}, \vec{r}') = K(x, x'; |\underline{v}' - \underline{v}|). \quad (2.11)$$

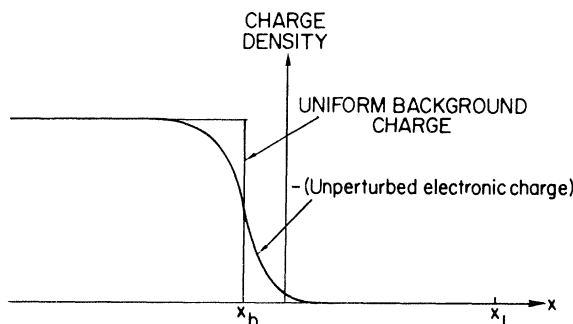


FIG. 1. Schematic representation of charge density in uniform-background model of a metal surface. External charges discussed in text are placed at x_1 , which is located well outside of the metal's electron distribution.

Substituting into (2.8) gives the equation

$$\rho(x; p) = \int K(x, x'; p) \psi(x'; p) dx', \quad (2.12)$$

where

$$\begin{aligned} K(x, x'; p) &= \int K(x, x'; v) e^{i\mathbf{p}\cdot\mathbf{v}} d^3v \\ &= 2\pi \int_0^\infty K(x, x'; v) J_0(pv) v dv \end{aligned} \quad (2.13)$$

and $v = |\mathbf{v}|$.

From (2.13) we deduce the following properties of the kernel $K(x, x'; p)$:

(a) Since by the nature of a metal the screening charge due to a point-perturbing potential located at \vec{r}' near the surface must be localized near \vec{r}' ,¹⁵ the kernel $K(\vec{r}, \vec{r}')$ is short ranged in $|\vec{r} - \vec{r}'|$, and hence $K(x, x'; p)$ is short ranged in $|x - x'|$.

(b) $K(x, x'; p)$ has a power-series expansion in even powers of p , obtained by expanding the Bessel function J_0 :

$$K(x, x'; p) = K_0(x, x') + p^2 K_2(x, x') + \dots \quad (2.14)$$

C. Self-Consistent Equations

To proceed further with (2.12), we write

$$\psi(x; p) = \psi^{\text{ext}}(x; p) + \Delta\psi(x; p). \quad (2.15)$$

The first term on the right-hand side is given by Eq. (2.6). The second term, due to the induced electron charge density, can be directly calculated from $\rho(\vec{r})$ [Eq. (2.10)] by Poisson's equation, resulting in

$$\psi(x; p) = (2\pi/p) [e^{-px_1} e^{px} + \int \rho(x'; p) e^{-p|x-x'|} dx'] \quad (2.16)$$

for x in the region of the metal. Equations (2.12) and (2.16) constitute the self-consistency problem for $\rho(x; p)$ and $\psi(x; p)$.

It is convenient to extract the dependence on x_1 explicitly by introducing the functions $\tilde{\psi}(x; p)$ and $\tilde{\rho}(x; p)$ through the following definitions:

$$\psi(x; p) = \tilde{\psi}(x; p) e^{-px_1}, \quad (2.17)$$

$$\rho(x; p) = \tilde{\rho}(x; p) e^{-px_1}. \quad (2.18)$$

Then the self-consistent equations (2.12) and (2.16) become

$$\tilde{\rho}(x; p) = \int K(x, x'; p) \tilde{\psi}(x'; p) dx', \quad (2.19)$$

$$\tilde{\psi}(x; p) = (2\pi/p) [e^{px} + \int \tilde{\rho}(x'; p) e^{-p|x-x'|} dx'], \quad (2.20)$$

in which x_1 no longer appears. Between these equations one can eliminate $\tilde{\psi}$, obtaining the following integral equation for $\tilde{\rho}$:

$$\begin{aligned} p\tilde{\rho}(x; p) &= 2\pi \int K(x, x'; p) [e^{px} \\ &+ \int \tilde{\rho}(x''; p) e^{-p|x'-x''|} dx''] dx'. \end{aligned} \quad (2.21)$$

III. METAL SURFACE IN UNIFORM FIELD

In Eq. (2.21) we now make the expansion

$$\tilde{\rho}(x; p) = \tilde{\rho}_0(x) + p\tilde{\rho}_1(x) + p^2\tilde{\rho}_2(x) + \dots \quad (3.1)$$

and equate equal powers of p [using expansion (2.14) for K]. This gives to order p^0 ,

$$0 = 2\pi \int K_0(x, x') dx' [1 + \int \tilde{\rho}_0(x'') dx'']. \quad (3.2)$$

Since $\int K_0(x, x') dx'$ represents the change in charge density at x due to a uniform change of potential and hence does not vanish,¹⁶ we must have

$$\int \tilde{\rho}_0(x'') dx'' = \int \rho(x''; 0) dx'' = -1. \quad (3.3)$$

This expresses the fact that an external uniform sheet of charge, at any distance x_1 from the surface, induces an equal and opposite total surface charge.

To order p^1 , we obtain, on recalling that K has no terms linear in p ,

$$\begin{aligned} \tilde{\rho}_0(x) &= 2\pi \int K_0(x, x') [x' - \int \tilde{\rho}_0(x'') |x' - x''| dx'' \\ &+ \int \tilde{\rho}_1(x'') dx''] dx'. \end{aligned} \quad (3.4)$$

Equations (3.4) and (3.3) determine the screening charge density $\tilde{\rho}_0(x)$ [= $\rho(x; 0)$] induced by a uniform external charge sheet, or, equivalently, by a uniform electric field. This is so in spite of the appearance in (3.4) of the unknown function $\tilde{\rho}_1(x)$. To determine $\tilde{\rho}_0(x)$, the integral

$$\lambda \equiv \int \tilde{\rho}_1(x'') dx'' \quad (3.5)$$

is first treated as a parameter, and a tentative function $\tilde{\rho}_0^{(\lambda)}(x)$ is found from Eq. (3.4). The value of λ is then varied until $\tilde{\rho}_0^{(\lambda)}(x)$ satisfies the normalization condition (3.3).

We have previously calculated the screening charge density $\rho(x; 0)$ (in Ref. 2) by solving directly the self-consistent equations of Kohn and Sham⁴ for a metal in a weak external electric field, and subtracting from the resulting charge density the unperturbed charge density. There is therefore no need to recalculate $\rho(x; 0)$ using the present self-consistent equations. Our earlier results are reproduced in Fig. 2. The Friedel oscillations of the screening charge, particularly for low bulk electron density (large r_s), are noteworthy. The figure also indicates the centers of mass,

$$x_0 = \int_{-\infty}^{\infty} x \rho(x; 0) dx / \int_{-\infty}^{\infty} \rho(x; 0) dx, \quad (3.6)$$

of the screening charge densities. Values of x_0 relative to x_b , the edge of the positive background, are listed in Table I. We recall here that, if the small lattice distortion is neglected (see Ref. 1, Appendix E),¹⁷ the last plane of ions is behind the edge of the uniform background, which models the lattice, by one-half of an interplanar spacing.¹

TABLE I. Positions x_0 of the center of mass of the induced surface charge density $\rho(x; 0)$ relative to the edge x_b of the uniform positive-charge background. r_s characterizes the bulk densities (see caption of Fig. 2). In determining x_0 , the Friedel oscillations in $\rho(x; 0)$ (Fig. 2) were extrapolated to $x = -\infty$, using their known asymptotic form (Ref. 1). Note that the numerical uncertainties in x_0 are small compared with a screening length (1 a. u. = 0.529 Å).

| r_s (a. u.) | $x_0 - x_b$ (a. u.) |
|------------------|------------------------|
| 2 | 1.6 ± 0.05 |
| 4 | 1.3 ± 0.2 |
| 6 | 1.2 ± 0.2 |

Thus the results in Table I permit locating x_0 for a metal relative to its lattice planes.

In the presence of a uniform, normal external electric field of magnitude \mathcal{E} pointing out of the metal, there is an induced charge density $\rho(x) = -(\mathcal{E}/4\pi)\rho(x; 0)$. Hence if we take the potential in the interior of the metal as unchanged by \mathcal{E} (for example, by grounding), Poisson's equation gives, for the corresponding change of the electrostatic potential,

$$\begin{aligned} \delta\psi(x) &\equiv \psi_{\mathcal{E}}(x) - \psi_0(x) \\ &= -4\pi \int_{-\infty}^x dx' \int_{-\infty}^{x'} dx'' \rho(x'') \\ &= \mathcal{E} \int_{-\infty}^x dx' \int_{-\infty}^{x'} dx'' \rho(x''; 0). \end{aligned} \quad (3.7)$$

The last double integral can be transformed by an integration by parts into

$$\delta\psi(x) = \mathcal{E} \int_{-\infty}^x (x - x') \rho(x'; 0) dx'. \quad (3.8)$$

Well on the inside of $\rho(x; 0)$, $\delta\psi$ is, by construction, zero; while well on the outside of $\rho(x; 0)$, we find by Eqs. (3.3) and (3.6),

$$\begin{aligned} \delta\psi(x) &= \mathcal{E} \int_{-\infty}^{\infty} (x - x') \rho(x'; 0) dx' \\ &= -\mathcal{E}(x - x_0). \end{aligned} \quad (3.9)$$

This may be compared with the result of classical electrostatics applied to a metal occupying the half-space $x < x_s$. Here $\delta\psi^{(cl)}$ vanishes for $x < x_s$, while for $x > x_s$,

$$\delta\psi^{(cl)}(x) = -\mathcal{E}(x - x_s). \quad (3.10)$$

Thus we see that, so far as a perpendicular external field is concerned, the point x_0 is to be regarded as determining the effective location of the metal surface.

IV. REFERENCE PLANE FOR IMAGE POTENTIAL

In this section, we shall show that for the purpose of computing the image potential of a point charge outside a metal surface, the effective location of the surface is again given by the x_0 of the

previous section [Eq. (3.6)].

We first must establish the preliminary result (4.5). For this purpose we return to the integral equation (3.4), with $\tilde{\rho}_0$ and $\tilde{\rho}_1$ defined by expansion (3.1), and let $x \rightarrow -\infty$. Deep in the metal, the screening charge $\tilde{\rho}_0(x) = \rho(x; 0)$ vanishes:

$$\lim_{x \rightarrow -\infty} \tilde{\rho}_0(x) = 0; \quad (4.1)$$

further, because of the short range of $K(x, x'; p)$ in $|x - x'|$ and the localization of $\tilde{\rho}_0(x'')$ near the surface, we may make the replacement, in Eq. (3.4),

$$|x' - x''| \rightarrow x'' - x'. \quad (4.2)$$

Substitution of (4.1) and (4.2) into (3.4) gives [using (3.3)]

$$\begin{aligned} 0 &= \int K_0(x, x') dx' [-\int \tilde{\rho}_0(x'') x'' dx'' \\ &\quad + \int \tilde{\rho}_1(x'') dx'']. \end{aligned} \quad (4.3)$$

Since, as remarked earlier, the first factor does not vanish, we have the identity

$$\int \tilde{\rho}_0(x'') x'' dx'' = \int \tilde{\rho}_1(x'') dx''. \quad (4.4)$$

The left-hand integral is just the first moment of $\tilde{\rho}_0(x)$. Hence, if we choose as the origin of our x axis the center of mass of $\tilde{\rho}_0(x)$, both terms in (4.4) vanish:

$$\int \tilde{\rho}_0(x'') x'' dx'' = \int \tilde{\rho}_1(x'') dx'' = 0. \quad (4.5)$$

We can now calculate the additional electrostatic energy due to the interaction of an external point charge q at $(x_1, 0, 0)$ with its induced surface charge. (It is easily seen, in the linear-response context, that the total additional energy due to the presence of the point charge differs from this by at most an additive constant, depending on the choice of the zero of energy.) We may write

$$\rho^{\text{ext}}(\vec{r}) = [q/(2\pi)^2] \delta(x - x_1) \int e^{i\vec{p}\cdot\vec{r}} d^2p. \quad (4.6)$$

The corresponding external potential and screening charge are, for $x < x_1$,

$$\psi^{\text{ext}}(\vec{r}) = (q/2\pi) \int (e^{-px_1/p}) e^{ipx} e^{i\vec{p}\cdot\vec{r}} d^2p, \quad (4.7)$$

$$\rho(\vec{r}) = [q/(2\pi)^2] \int e^{-px_1} \tilde{\rho}(x; p) e^{i\vec{p}\cdot\vec{r}} d^2p. \quad (4.8)$$

The interaction energy is

$$\begin{aligned} U &= \frac{1}{2} \int \psi^{\text{ext}}(\vec{r}) \rho(\vec{r}) d^3\vec{r} \\ &= (q^2/4\pi) \int d^2p (e^{-2px_1/p}) \int dx e^{px} \tilde{\rho}(x; p). \end{aligned} \quad (4.9)$$

Now, in view of (3.3) and (4.5),

$$\begin{aligned} &\int dx e^{px} \tilde{\rho}(x; p) \\ &= \int dx (1 + px + \frac{1}{2}p^2x^2 + \dots) [\tilde{\rho}_0(x) + p\tilde{\rho}_1(x) \\ &\quad + p^2\tilde{\rho}_2(x) + \dots] \end{aligned}$$

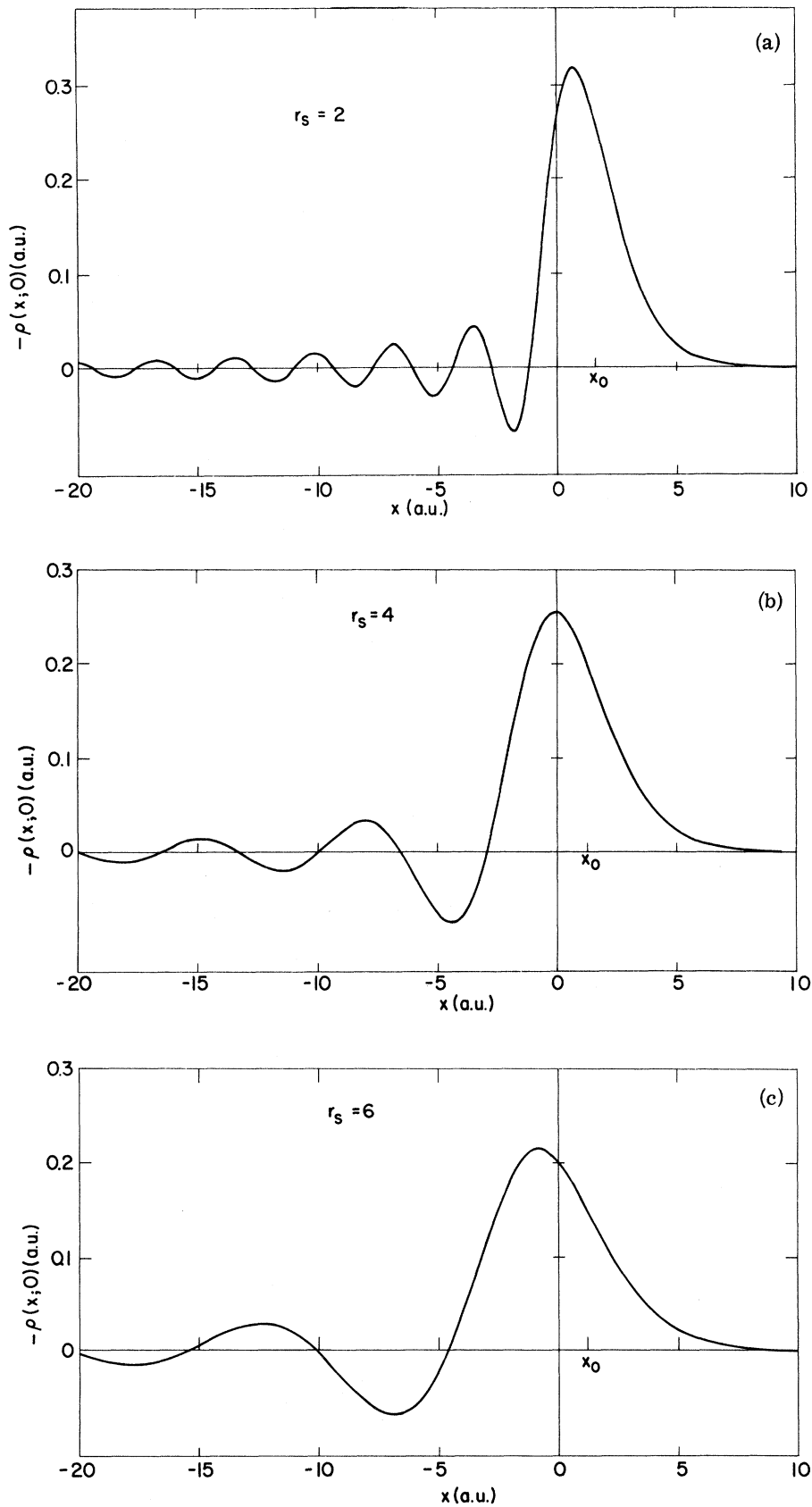


FIG. 2. Profiles of induced surface charge density $\rho(x; 0)$. x and ρ are measured in atomic units ($|e| = m = \hbar = 1$); the atomic unit of length is 0.529 Å. Note that $\rho(x; 0)$ satisfies the normalization condition Eq. (3.3). r_s characterizes the bulk densities ($\frac{4}{3}\pi r_s^3 \equiv -\rho_e^{-1}$, with ρ_e the bulk electronic charge density, in atomic units). The edge of the uniform positive-charge background, x_b , is taken at the origin. x_0 , the center of mass of $\rho(x; 0)$, is shown in the text to be the effective location of the metal surface. (These density distributions are the same as those given in Ref. 2, except for some very small differences arising from use in the present computation of somewhat weaker fields.)

$$\begin{aligned}
&= \int dx \bar{\rho}_0(x) + p \left[\int dx x \bar{\rho}_0(x) + \int dx \bar{\rho}_1(x) \right] + \dots \\
&= -1 + \gamma p^2 + \dots, \quad (4.10)
\end{aligned}$$

where γ is some constant of the order of an atomic dimension squared. An essential feature of (4.10) is the absence of a term linear in p .

When (4.10) is substituted into (4.9), one obtains

$$\begin{aligned}
U &= (q^2/4\pi) \int_0^\infty 2\pi p dp (e^{-2px_1}/p) (-1 + \gamma p^2 + \dots) \\
&= q^2 \left(-\frac{1}{4x_1} + \frac{\gamma}{8x_1^3} + \dots \right), \quad (4.11)
\end{aligned}$$

or, if we revert to an arbitrary origin of the x axis,

$$U = -\frac{q^2}{4(x_1 - x_0)} + O\left(\frac{q^2}{(x_1 - x_0)^3}\right). \quad (4.12)$$

This is the classical image potential referred to the plane passing through x_0 , which thus is again to be regarded as the effective location of the metal surface.

We remark that x_0 is identical to the x coordinate \bar{x}_0 of the center of mass of the image charge:

$$\begin{aligned}
\bar{x}_0 &= \frac{\int x \rho(\vec{r}) d^3\vec{r}}{\int \rho(\vec{r}) d^3\vec{r}} = \frac{\int d^2p \int x \rho(x; p) dx \int e^{i\vec{p}\cdot\vec{r}} d^2v}{\int d^2p \int \rho(x; p) dx \int e^{i\vec{p}\cdot\vec{r}} d^2v} \\
&= \frac{\int x \rho(x; 0) dx}{\int \rho(x; 0) dx} = x_0. \quad (4.13)
\end{aligned}$$

Finally, we note that in view of the results of this section and Sec. III, the potential energy of a small point charge q at x_1 well outside the surface, in the presence of a weak uniform electric field of magnitude \mathcal{E} pointing out of the metal, is given by

$$\text{const} - \frac{q^2}{4(x_1 - x_0)} - q\mathcal{E}(x - x_0') \quad (4.14)$$

with $x_0' = x_0$.¹⁸

V. APPLICATIONS

A. Alkali Adsorption

In this subsection we use the results obtained above to discuss the substrate-adsorbate separation for an alkali atom chemisorbed on a metal surface.¹⁹ Let us denote the distance between the center of the alkali ion and the plane through the centers of the last layer of substrate ions by s , and that between the center of the alkali ion and the effective metal surface at x_0 by a (see Fig. 3).

We begin by imagining that the alkali atom is far from the metal surface. We then transfer its valence electron to the substrate. The additional charge acquired by the substrate will, of course, be concentrated near its surface. Because the ion is far away, the screening charge can be calculated by linear-response theory, and so, in accordance

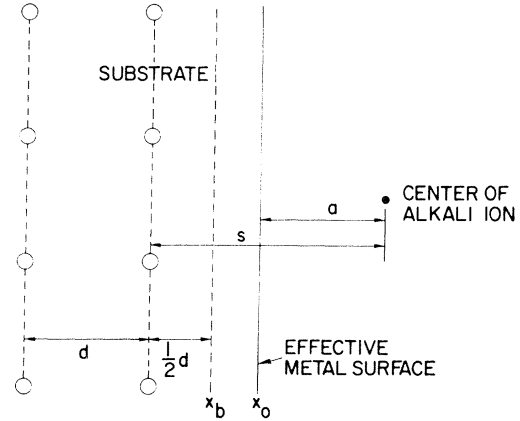


FIG. 3. Spatial configuration associated with alkali atom adsorbed on a single-crystal metal substrate. Open circles represent positions of centers of substrate ions. Dashed line at x_b gives edge of uniform positive background used to model the substrate ionic lattice; solid line at x_0 gives location of effective metal surface. Various distances marked are discussed in the text.

with our previous discussion [cf. Eq. (4.13)], the center of gravity of the additional charge will be at x_0 . The combination of this charge and the ion has a dipole moment $\vec{\mu}$, pointing along the outward normal to the surface, with magnitude²⁰

$$\mu = Za. \quad (5.1)$$

Here Z is the adsorbate ionic charge, equal to 1 in the present case.

We will determine the location of x_0 for the substrate crystal, as discussed previously, by replacing its ionic lattice by a uniform positive background terminated at a plane. If this plane is located at $x = x_b$, then, as noted earlier, the last layer of substrate ions (i.e., the plane through the ion centers) is at $x = x_b - \frac{1}{2}d$, with d the interplanar spacing. Hence, with $Z = 1$,

$$s = \mu + (x_0 - x_b) + \frac{1}{2}d \quad (5.2)$$

(see Fig. 3).

We now allow the ion to move in toward its equilibrium s value. If its final position is too close to the surface, nonlinear effects will become significant,²¹ as will the atomic "roughness" of the surface. We will, however, assume that this response remains linear, and will therefore confine our attention to the alkali ions of largest radius, K and Cs (there is little relevant experimental data on Rb), which are presumably farthest out from the surface. We will also consider only adsorption on the most closely packed crystal face of the substrate, since this face presents to the adsorbate an electron density most like that of the plane-terminated uniform-background model, with

its absence of variation parallel to the surface.²²

Now the ionization potentials I of Cs and K are ~ 4 eV, while the work functions ϕ of the most closely packed faces of the transition-metal substrates generally used in alkali-adsorption experiments are ~ 5 eV. Hence if the valence level of the alkali neither shifted nor broadened when the ion was brought in toward the surface, this level would remain empty. It does broaden, however,²³⁻²⁹ and since part of this broadened level will be below the substrate Fermi energy, it becomes partly filled. The level also shifts upward in energy,^{24,26,28,29} which of course decreases its tendency to fill. The degree to which the level remains unfilled (in the alkalis) is sometimes described very crudely by using a $Z_{\text{eff}} < 1$ in Eq. (5.1). The analyses now in the literature obtain Z_{eff} values not far from unity ($Z_{\text{eff}} \gtrsim 0.8$)^{24,26,30} for K and Cs adsorption on the high-work-function substrates of interest. We will neglect these effects here, take $Z_{\text{eff}} = 1$ (which would probably not be a good approximation for Na or Li adsorption), and use Eq. (5.2) to obtain equilibrium s values for K and Cs from experimental data on μ .

Table II gives such data for adsorption on the most closely packed faces of W, Ta, and Re. Since these substrates all have very high electron densities, the $(x_0 - x_b)$ value corresponding to $r_s = 2$ in Table I was used to compute s . It should be recognized that it is a very crude approximation to describe a transition metal by using a uniform-background model. The corresponding s values, which are in the range 6.4–7.6 a.u. (1 a.u. = 0.529 Å) are given in the table.

There are practically no experimental measurements of s at the present time. Andersson and Kasemo³¹ have estimated from results on the specular reflection of low-energy electrons by a Ni(100) surface covered with layers of K and of Cs, that $s = 6.7$ and 7.2 a.u., respectively. The alkali coverage in this experiment was about $\frac{1}{3}$ – $\frac{1}{2}$ of a full layer, however, rather than the very low coverage to which our discussion would be applicable; and in addition the interpretation of the experiment is quite difficult.

Unfortunately there do not now exist measurements of both μ and s for the closest-packed face of the same metal and a heavy adsorbed alkali atom. Such measurements would be of great interest.

We turn now briefly to the heat of desorption.³² We denote by E_+ the heat of ionic desorption in the low-coverage limit, which is related to the heat of atomic desorption, E_0 , by $E_+ - E_0 = I - \phi$. If linear-response theory is adequate, we should have

$$E_+ = (4\mu)^{-1}, \quad (5.3)$$

where we neglect the energy of substrate-adsor-

bate repulsion because of the short range of the repulsive interaction (cf. Born–Mayer theory of alkali halides). Table III compares values for E_+ and $(4\mu)^{-1}$ obtained from measured E_0 and μ values; the agreement is reasonable. Note that this agreement also provides a crude experimental verification of our proof that the image-potential reference plane is at the same location as the center of mass of the induced charge.

B. Effective Spacing of Condenser Plates

Here we discuss the relevance of our results to the determination of the effective plate spacing of a parallel-plate condenser.³³ We take the parallel faces to be normal to the x axis, with plate a located further along the positive x direction than plate b . The plates are assumed initially to be in equilibrium with one another. (This means that if the work functions of the two faces differ, there will be a contact difference of potential between them, and an associated surface charge; the chemical potentials will be equal.)

We connect the positive terminal of a battery of potential V to plate a and the negative terminal to plate b , raising the mean interior electrostatic potential of plate a by an amount V with respect to that of plate b , and inducing an additional surface charge σ per unit area on face a (and $-\sigma$ per unit area on face b). The capacitance per unit area is

TABLE II. Calculated distance s between center of adsorbed alkali ion and last substrate lattice plane. μ is zero-coverage dipole moment (see Ref. 20); d is substrate interplanar spacing (1-a.u. length = 0.529 Å; 1-a.u. energy = 27.2 eV).

| Adsorbate/Substrate | μ (a. u.) | d (a. u.) | s (a. u.) |
|---------------------|------------------|----------------|----------------|
| Cs/Ta (110) | 3.0 ^a | 4.4 | 6.8 |
| Cs/W (110) | 3.9 ^b | 4.2 | 7.6 |
| Cs/Re (0001) | 3.2 ^c | 4.2 | 6.9 |
| K/Ta (110) | 2.6 ^a | 4.4 | 6.4 |
| K/W (110) | 3.1 ^d | 4.2 | 6.8 |

^aD. L. Fehrs and R. E. Stickney, *Surface Sci.* **24**, 309 (1971).

^bT. J. Lee, B. H. Blott, and B. J. Hopkins, *J. Phys. F* **1**, 309 (1971). Data obtained using the field-emission method of Swanson and Strayer [*J. Chem. Phys.* **48**, 2421 (1968)], Sidorski, Pelly, and Gomer [*J. Chem. Phys.* **50**, 2382 (1969)], and Gavriluk, Naumovets, and Fedorus [*Zh. Eksperim. i Teor. Fiz.* **51**, 1332 (1966) [*Sov. Phys. JETP* **24**, 899 (1967)]] have not been used because of problems related to determination of coverage values that appear at present not fully to be resolved.

^cD. L. Fehrs and M. S. Macrakis, *Bull. Am. Phys. Soc.* **15**, 391 (1970); and private communication.

^dL. D. Schmidt and R. Gomer, *J. Chem. Phys.* **45**, 1605 (1966).

TABLE III. Comparison of E_* with $(4\mu)^{-1}$. μ is measured zero-coverage dipole moment (see Ref. 20). E_* is ionic desorption energy computed from atomic desorption energy: $E_* = E_0 + I - \Phi$. (I is ionization potential, Φ is substrate work function.) a. u. \equiv atomic units (1-a. u. length = 0.529 Å; 1-a. u. energy = 27.2 eV). Recent E_0 data were not available for all of the substrate/adsorbate combinations in Table II.

| Adsorbate/Substrate | E_0 (a. u.) | μ (a. u.) | I (a. u.) | Φ (a. u.) | E_* (a. u.) | $(4\mu)^{-1}$ (a. u.) |
|---------------------|--------------------------|------------------|----------------|--------------------|------------------|--------------------------|
| Cs/W (110) | 0.103–0.121 ^a | 3.9 ^b | 0.143 | 0.189 ^c | 0.057–0.075 | 0.064 |
| K/W (110) | 0.107 ^d | 3.1 ^b | 0.159 | 0.189 ^c | 0.077 | 0.081 |

^aL. W. Swanson and R. W. Strayer, NASA Final Report No. NGR 38-010-001, 1970 (unpublished) (2.8 eV); V. M. Gavriilyuk, Yu. S. Vedula, A. G. Naumovets, and A. G. Fedorus, Fiz. Tverd. Tela **9**, 1126 (1967) [Sov. Phys. Solid State **9**, 881 (1967)] (3.2 eV); Z. Sidorski, I. Pelly, and R. Gomer, J. Chem. Phys. **50**, 2382 (1969) (3.3 eV).

^bSee Table II.

^cT. J. Lee, B. H. Blott, and B. J. Hopkins, J. Phys. F **1**, 309 (1971) (5.14 eV, measured by contact-potential-difference technique).

^dL. D. Schmidt and R. Gomer, J. Chem. Phys. **45**, 1605 (1966) (2.9 eV).

$$C = \sigma/V. \quad (5.4)$$

If we denote the change in charge density on plate i by $\rho^{(i)}(x)$, then

$$\int_{-\infty}^{\infty} \rho^{(a)}(x) dx = - \int_{-\infty}^{\infty} \rho^{(b)}(x) dx = \sigma, \quad (5.5)$$

and, using Poisson's equation to calculate the difference in mean interior electrostatic potential between the plates,

$$V = 4\pi \int_{-\infty}^{\infty} x[\rho^{(a)}(x) + \rho^{(b)}(x)] dx. \quad (5.6)$$

Equations (5.4)–(5.6) and (3.6) imply Eq. (1.2); i. e., the effective plate spacing l_c for capacitive effects is

$$l_c \equiv (4\pi C)^{-1} = x_0^{(a)} - x_0^{(b)}. \quad (5.7)$$

For simplicity of presentation, we now take the two plates to be of the same material and the two inside parallel faces to have the same crystallographic orientation (with corresponding interplanar spacing d). Then if l is the distance between the closest two lattice planes on opposite sides of the condenser gap from one another (see Fig. 4),

$$l_c = l - 2(x_0 - x_b) - d, \quad (5.8)$$

with $x_0 - x_b$ given in Table I. (x_0 and x_b refer to a metal oriented as in Fig. 1; i. e., $x_0 - x_b = x_0^{(b)} - x_b^{(b)}$.)

There have been no measurements of l for small-gap condensers, and thus there is no data with which to compare Eq. (5.8) in a direct way. There have, however, been experimental studies of the tunneling properties of such condensers,^{34–38} and the measurements have been interpreted in terms of a plate separation l_t . Examination of the theories³⁹ used in these interpretations indicates that l_t is to be identified with the distance between the closest classical turning points for the two plates.⁴⁰ (A turning point, whose location is denoted x_t , is a point on the x axis at which the

Fermi level crosses the curve of total effective potential seen by a Fermi-level electron.) Since $x_0^{(a)} - x_t^{(a)} = x_t^{(b)} - x_0^{(b)}$, we have

$$l_c = l_t + 2(x_t - x_0), \quad (5.9)$$

with x_0 and x_t referring to a metal oriented as in Fig. 1 (i. e., $x_t - x_0 = x_t^{(b)} - x_0^{(b)}$). Thus at $r_s = 2$, for which $x_t - x_0 = 0.8$ a. u. (see Table I and Ref. 1), $l_c - l_t = 1.6$ a. u.; i. e., the capacitive separation exceeds the tunneling separation by nearly 1 Å. The findings of Mead³⁴ ($l_c - l_t \approx 2.75$ Å for a Ta-Ta₂O₅-Au junction) are suggestive of such a result, but a number of later studies^{35,37} indicate the importance of factors like unevenness of the plate surfaces in interpreting the experiment (tunneling of course emphasizes the regions of smallest plate separation).

C. Field Emission

Here we discuss briefly the relevance of a field-emission experiment to verifying the equality of x_0 and x_0' in Eq. (4.14). The electrons leaving the

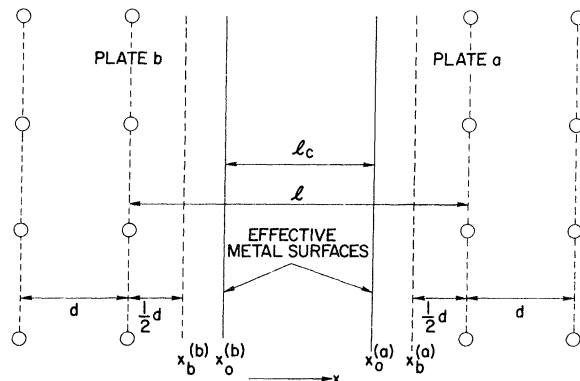


FIG. 4. Spatial configuration associated with two identical metal single crystals forming a parallel-plate condenser (see caption of Fig. 2).

emitter surface in this experiment are of course dynamical objects, while our theory of the image potential is designed for classical static charges. It has been shown by Rudnick,⁸ however, that slow electrons well outside a metal surface experience the same potential as such a static charge, and so we may write the potential energy (relative to the Fermi level) of a field-emitted electron in this region as⁴¹

$$\Phi - \frac{1}{4(x-x_0)} - \mathcal{E}(x-x'_0) \quad (5.10)$$

(the emitter surface is oriented as in Fig. 1). Here Φ is the emitter work function, \mathcal{E} is the magnitude of the field (which points into the metal), and we assume for the moment (contrary to our earlier discussion) that $x'_0 \neq x_0$. Note that this potential energy has a maximum value

$$\epsilon_{\max} = \Phi - \mathcal{E}^{1/2} - \mathcal{E}(x_0 - x'_0). \quad (5.11)$$

Measurements of total energy distribution curves at a variety of \mathcal{E} values have been reported for field emission from a heated tip.⁴²⁻⁴⁴ The theoretical analysis of the experiment, as noted by Gadzuk and Plummer,⁴⁴ shows that the curves will exhibit a change in slope at energy ϵ_{\max} , where the emission mechanism changes from tunneling to thermionic emission, thus permitting determina-

tion of ϵ_{\max} .

The most straightforward way of using such results to test the equality of x_0 and x'_0 would be to extract a curve of ϵ_{\max} vs \mathcal{E} and determine the coefficient of the linear component [Eq. (5.11)]. The reported data unfortunately are not complete enough to permit a meaningful analysis of this sort.

VI. CONCLUDING REMARKS

We would like to add two comments here. In Sec. II we stated that we would justify treating the positive ions as undisplaced by the external field. From the electronic screening charge distributions shown in Fig. 2, we can now in fact verify that at the position of the ions, the external field has been largely screened out. For example, for the most closely packed [(110)] face of Na, this screening is over 95% effective.⁴⁵

Second, we would like to refer to the forthcoming paper of Appelbaum and Hamann.¹⁴ They remark that the position of the center of mass of the image charge is qualitatively similar to the reference plane for the image potential. In the present paper we have seen that these two quantities are formally identical, and thus the small discrepancy found by these authors must be due to approximations in their variational calculation.⁴⁶

*Supported in part by the Office of Naval Research and the National Science Foundation.

¹N. D. Lang and W. Kohn, Phys. Rev. B **1**, 4555 (1970).

²N. D. Lang and W. Kohn, Phys. Rev. B **3**, 1215 (1971).

³P. Hohenberg and W. Kohn, Phys. Rev. **136**, B864 (1964).

⁴W. Kohn and L. J. Sham, Phys. Rev. **140**, A1133 (1965).

⁵These profiles were previously calculated by us (Ref. 2) in the context of the theory of the work function.

⁶"External" is understood in the sense of well outside the surface electron charge cloud.

⁷D. M. News, Phys. Rev. B **1**, 3304 (1970).

⁸J. Rudnick, Ph.D. thesis (University of California, San Diego, 1970) (unpublished); Phys. Rev. B **5**, 2863 (1972).

⁹D. E. Beck and V. Celli, Phys. Rev. B **2**, 2955 (1970).

¹⁰L. I. Schiff, Phys. Rev. B **1**, 4649 (1970). See also V. E. Kenner, R. E. Allen, and W. M. Saslow, Phys. Lett. **38A**, 255 (1972).

¹¹P. J. Feibelman, Surf. Sci. **27**, 438 (1971).

¹²V. Peuckert, Z. Phys. **241**, 191 (1971).

¹³Cf. also P. A. Fedders, Phys. Rev. **153**, 438 (1967); J. C. Inkson, Surf. Sci. **28**, 69 (1971); J. A. Appelbaum and G. A. Baraff, Phys. Rev. B **4**, 1246 (1971); D. M. News, J. Chem. Phys. **50**, 4572 (1969); J. Bardeen, Phys. Rev. **58**, 727 (1940).

¹⁴Other calculations dealing with different aspects of the surface screening problem, including many-body effects, that were performed approximately simultaneously with the present calculation, are S. C. Ying, J. R. Smith, and W. Kohn [J. Vac. Sci. Technol. **9**, 575 (1972)] and J. A. Appelbaum and D. R. Hamann [Phys. Rev. B **6**, 1122 (1972)].

¹⁵This can be easily verified if \vec{r}' is in the metal interior, but we don't know of a formal proof when \vec{r}' is near the surface.

¹⁶In the interior of the metal this change can be easily calculated in term of the chemical potential.

¹⁷See also P. M. Marcus, D. W. Jepsen, and F. Jona, Surface Sci. **31**, 180 (1972); G. E. Laramore and C. B. Duke, Phys. Rev. B **5**, 267 (1972); C. B. Duke, G. E. Laramore, B. W. Holland, and A. M. Gibbons, Surf. Sci. **27**, 523 (1971).

¹⁸Occasionally it has been suggested that x_0 and x'_0 need not be identical. See, e.g., T. T. Tsong and E. W. Müller, Phys. Rev. **181**, 530 (1969).

¹⁹The discussion is confined to the extreme low-coverage limit. For an analysis of alkali adsorption at arbitrary coverages, from a somewhat different point of view, see N. D. Lang [Phys. Rev. B **4**, 4234 (1971)].

²⁰This is generally determined experimentally by studying, as a function of the number N of adsorbed alkali atoms per unit area, the work function $\Phi(N)$ of the alkali-covered metal. The magnitude of the moment μ is given by $-(4\pi)^{-1}d\Phi/dN$ for $N \rightarrow 0$. Some writers discuss a moment defined as $-(2\pi)^{-1}d\Phi/dN$, but this is not appropriate here.

²¹Cf. J. A. Appelbaum and D. R. Hamann, Ref. 14.

²²Cf. R. Smoluchowski, Phys. Rev. **60**, 661 (1941).

²³R. W. Gurney, Phys. Rev. **47**, 479 (1935).

²⁴A. J. Bennett and L. M. Falicov, Phys. Rev. **151**, 512 (1966).

²⁵L. D. Schmidt and R. Gomer, J. Chem. Phys. **45**, 1605 (1966).

²⁶J. W. Gadzuk, in *Structure and Chemistry of Solid Surfaces*, edited by G. A. Somorjai (Wiley, New York, 1969).

²⁷T. B. Grimley, J. Vac. Sci. Technol. **8**, 31 (1971).

²⁸M. Remy, J. Chem. Phys. **53**, 2487 (1970).

²⁹Cf. also D. M. News, Phys. Rev. **178**, 1123 (1969); J. R. Schrieffer, J. Vac. Sci. Technol. **9**, 561 (1972).

³⁰K. F. Wojciechowski, Acta Phys. Pol. **29**, 119 (1966); Acta

Phys. Pol. **33**, 363 (1968)

³¹S. Andersson and B. Kasemo, *Surface Sci.* **32**, 78 (1972).

³²Cf. desorption-energy calculation of J. W. Gadzuk, J. K. Hartman, and T. N. Rhodin [*Phys. Rev. B* **4**, 241 (1971)].

³³H. Y. Ku and F. G. Ullman [*J. Appl. Phys.* **35**, 265 (1964)] considered this problem earlier. A difficulty with their treatment is that the concept of a metal "surface" is introduced without a microscopic definition. The effective plate spacing is discussed in terms of electric-field "penetration" into the plates by a finite distance past their surfaces. {Other discussions of such static-field penetration effects have been given by O. K. Rice, [*Phys. Rev.* **31**, 1051 (1928)]; N. F. Mott and R. J. Watts-Tobin [*Electrochim. Acta* **4**, 79 (1961)]; and T. T. Tsong and E. W. Müller [Ref. 18].} In the present treatment, the definition and actual position of the surface is specified precisely. (The analog here of "penetration" effects is of course just the fact that the induced charge distributions, as in Fig. 2, have a finite width.)

³⁴C. A. Mead, *Phys. Rev. Lett.* **6**, 545 (1961).

³⁵R. M. Handy, *Phys. Rev.* **126**, 1968 (1962).

³⁶J. L. Miles and P. H. Smith, *J. Electrochem. Soc.* **110**, 1240 (1963)

³⁷K. H. Gundlach and G. Heldmann, *Solid State Commun.* **5**, 867 (1967).

³⁸J. Bernard, G. Delacote, and Y. Mentalecheta, *Phys. Status Solidi* **31**, 315 (1969)

³⁹E.g., J. G. Simmons, *J. Appl. Phys.* **34**, 1793 (1963).

⁴⁰A correction for the image potential seen by the tunneling electron is sometimes included in these analyses. The image plane and turning point are generally taken to be at the same location, which, according to Table I and Ref. 1, is not quite correct.

⁴¹P. H. Cutler and J. J. Gibbons [*Phys. Rev.* **111**, 394 (1958)] and G. G. Belford, A. Kuppermann, and T. E. Phipps [*Phys. Rev.* **128**, 524 (1962)] have studied the periodic deviations in the Schottky effect using a potential which tends toward (5.10) for large x , with $x'_0 - x_0$ (equal to their parameter η) nonzero. The important feature of this potential, however, is probably not the $x'_0 \neq x_0$ feature of the asymptotic form, but rather the behavior of the potential in the immediate region of the surface, where (with $\eta \neq 0$) it exhibits a minimum. This same potential was used later by P. H. Cutler and D. Nagy [*Surf. Sci.* **3**, 71 (1964)] in studying field emission.

⁴²R. D. Young and E. W. Müller, *Phys. Rev.* **113**, 115 (1959).

⁴³L. W. Swanson and L. C. Crouser, *Phys. Rev.* **163**, 622 (1967).

⁴⁴J. W. Gadzuk and E. W. Plummer, *Phys. Rev. B* **3**, 2125 (1971).

⁴⁵As measured at the ion centers.

⁴⁶Since submission of this paper, two publications dealing with the same general subject have appeared: G. Paasch, H. Eschrig, and W. John, *Phys. Status Solidi B* **51**, 283 (1972); A. K. Theophilou and A. Modinos, *Phys. Rev. B* **6**, 801 (1972).

Defect Energetics for Self-Diffusion in Sodium*

Paul S. Ho[†]

Cornell University, Ithaca, New York 14850

and Argonne National Laboratory, Argonne, Illinois 60439

(Received 11 September 1972)

Recent data on self-diffusion and the isotope effect in sodium indicate clearly the existence of at least two operating defect mechanisms. This paper investigates the possibility of vacancy, divacancy, and interstitial mechanisms by calculating the diffusion energetics for the vacancy-type defects and estimating the same for interstitials based on other calculations. The aim is to search for a combined mechanism which can be used to interpret the available data on defect studies. The validity of choosing pseudopotentials for defect calculations is tested by using three potentials with different exchange and correlation corrections in the dielectric function of the conduction electrons. There is about a 15% variation in the results for vacancy and divacancy. Our energetic results indicate that a combined vacancy and divacancy mechanism can be used to account for most of the data obtained in diffusion, isotope effect, and dilatometric measurements. The available theoretical and experimental results do not seem to favor, but cannot completely rule out, the interstitial mechanism. It is suggested that the question is not likely to be resolved by further energetic calculations due to the lack of reliable interatomic potentials at close ranges; instead, experiments designed for detecting interstitials and dynamical calculations of ΔK are needed.

I. INTRODUCTION

Currently there is considerable interest in studying diffusion and defect energetics in sodium. The primary objective of these investigations is to gain a basic understanding of the diffusion mechanisms operative in bcc metals by studying a typical simple metal, such as sodium. The experimental studies cover a variety of techniques, such as dif-

fusion measurements,^{1,2} isotope effects,^{1,2} dilatometric measurement,³ NMR,⁴ cold-work annealing,⁵ defect-resistivity measurement,⁶ and defect-specific-heat measurement.⁷ Some of these experiments have been carried out over extensive ranges of pressure and temperature. In Table I, the results of most of these experiments are summarized. The following characteristics, which are important to the study of diffusion mechanisms in